archaeometry

Archaeometry **53**, 4 (2011) 693–706 doi: 10.1111/j.1475-4754.2010.00572.x

CHARACTERIZATION OF PLASTERS FROM PTOLEMAIC BATHS: NEW EXCAVATIONS NEAR THE KARNAK TEMPLE COMPLEX, UPPER EGYPT*

H. H. MAREY MAHMOUD† and M. F. ALI

Department of Conservation, Faculty of Archaeology, Cairo University, 12613 Giza, Egypt

E. PAVLIDOU

Physics Department, Aristotle University, 54124 Thessaloniki, Greece

N. KANTIRANIS

Department of Mineralogy–Petrology–Economic Geology, Aristotle University, 54124 Thessaloniki, Greece

and A. EL-BADRY

The Supreme Council of Antiquities in Egypt (SCA), Luxor, Egypt

The aim of the present work is to characterize plasters from Ptolemaic baths recently discovered in front of the Karnak temple complex, by the excavations of an Egyptian–French team. The characterization was carried out by means of optical microscopy (OM), scanning electron microscopy (SEM) equipped with an energy-dispersive X-ray detector (EDS), X-ray diffraction analysis (XRD) and Fourier transform infrared spectroscopy (FT–IR). The results allowed the identification of the chemical composition and structure of these plasters. In addition, samples of red, yellow, black and white pigments were examined and identified. The results helped in providing an image concerning some materials used during the Ptolemaic era in ancient Egypt.

KEYWORDS: PLASTERS, PTOLEMAIC BATHS, THE KARNAK TEMPLE COMPLEX, SEM–EDS, XRD, FT–IR, CALCITE, ARAGONITE, BONE BLACK

INTRODUCTION

The Ptolemaic period began with the invasion of ancient Egypt by Alexander the Great in 333 BC. Ptolemy (303 to 285 BC) was one of Alexander the Great's most trusted generals, and he worked on the promotion of a new Hellenized Egypt, centred in Alexandria (Ellis 1994). The Karnak temple complex is one of the largest monuments in the world, containing approximately 20 minor temples. The temple is located about 2.5 km to the north of Luxor and about 670 km south of Cairo. It is dated from the New Kingdom (the 18th Dynasty, 1540 to 1292 BC) until the late periods in Egypt, although new excavations have indicated an origin in the Old Kingdom (2575 to 2465 BC). According to Blyth (2006), statues attributed to kings of the Archaic and Old Kingdom periods—Khasekhemui (Dynasty II), Khufu (Dynasty IV) and Neuserre (Dynasty V)—are used to argue for the existence of a form of sanctuary or temple at

*Received 15 June 2010; accepted 5 November 2010
†Corresponding author: email marai79@hotmail.com

Karnak dating back to at least the Old Kingdom. Moreover, it is certainly believed by some scholars that the earliest occupation of the site appears to be from the First Intermediate Period (2160 to 2055 BC) (Gabolde *et al*. 1999; Gabolde 2000). This is clearly seen in the recent (2007) excavations of Marie Millet, to the south-east of the sacred lake (Bunbury *et al*. 2008).

The baths

The recent excavations by an Egyptian–French team in front of the Karnak temple complex led to the complete exposure of two Ptolemaic baths. The Supreme Council of Antiquities in Egypt (SCA) moved the village of El-Hassassna, which was located to the north-west of Karnak. There, an embankment and Roman settlements close to the Ptolemaic baths were discovered (http://www.cfeetk.cnrs.fr/uk/index.php).

Subsequently, a large wall was discovered and the Nile sediments found in front of it indicate the presence of an embankment and the fact that the Nile was coming right up to the front of Karnak. A jar containing a total of 316 coins was found, dated back to the reign of Ptolemy III (246 to 221 BC). The circular Ptolemaic bath contains an intricate mosaic tiled floor and seating for 16 people, with seats flanked by dolphin statuettes (Fig. 1). Public baths were a feature of Greek life and a version of the modern Egyptian coffee shop; and men would meet and do business in them. There was a gymnasium at Herakleopolis Magna (Ihnasya el-Medina), which seems to have used exclusively by the Greek soldier settlers in the first century BC (McKenzie 2007).

Research aims

In general, there are few published data on the ancient materials used during the Ptolemaic era in Egypt (Abd El Hady 2000; El Goresy 2000; Mao 2001; Ali 2003; Kieser *et al*. 2004; Tchapla *et al*. 2004; Shortland and Tite 2005; Ashton 2008; Marey Mahmoud 2009). Because of this, the first research task was devoted to characterizing plaster samples collected from Ptolemaic baths recently discovered in excavations near the Karnak temple complex. The analytical techniques utilized in this work were optical microscopy (OM), scanning electron microscopy (SEM) equipped with an energy-dispersive X-ray detector (EDS), X-ray diffraction analysis (XRD) and Fourier transform infrared spectroscopy (FT–IR). The second research task was to identify the colour palette used for decoration of these plasters and to determine the painting technique. Fifteen plaster samples were chosen for analytical studies concerning the following questions:

1. Do the plaster layers applied in the Ptolemaic baths match in their structure and chemical composition with those from Pharaonic and Roman times?
2. What are the materials used in the construction of the Ptolemaic baths and the technologies used to improve their resistance to water?
3. What are the novelties and the modifications in the chromatic palette and the painting techniques used in the Ptolemaic age?

The results of this study bring us much information on materials and technologies used during the Ptolemaic age, and particularly the materials used in the baths and similar constructions. The results will be used for the conservation–restoration interventions regarding the baths.

Figure 1 *(a) A general view of the Ptolemaic baths in front of the Karnak temple complex. (b) A detail of an individual seat in one of the Ptolemaic baths. (c) A wall plastered with a lime-based plaster. (d) A detail of the painted plaster layers.*

METHODOLOGIES

Samples

As a result of the burial environment and the deterioration factors following the excavations, a large number of detached painted fragments were found at the site. Fifteen (15) tiny samples of the detached plaster layers (with approximate dimensions 2×4 to 5×8 cm) were carefully chosen for analysis. Also, very small representative pigment samples (a few milligrams) were carefully scraped off the painted walls with a metallic scalpel from areas showing a good state of preservation.

The analytical methodology

In this work, the analytical techniques utilized to study the plaster samples were OM, SEM–EDS, XRD and FT–IR spectroscopy. In order to identify the stratigraphy of the plaster layers, some cross-sections were examined using a stereomicroscope.

Optical microscopy

Analysis of cultural materials and in particular the painted objects usually begins with a visual investigation of the surface. The stratigraphical structure of the plaster layers was examined using a Zeiss (stemi DV4) stereomicroscope with a Sony camera (DSC-S85).

Scanning electron microscopy with an EDS microanalysis detector (SEM–EDS)

The microstructure and the morphological characteristics were determined using a JEOL JSM-840A scanning electron microscope in the backscattered electrons mode (BSE). The microanalysis was carried out using an energy-dispersive X-ray (EDS) Oxford ISIS 300 microanalytical system, with a detection limit of less than 1% depending on the element. The accelerating voltage was 20 kV, probe current 45 nA, the working distance 20 mm and the counting time 60 s real time. The matrix correction protocol was ZAF correction. The samples were coated with carbon, using a Jeol JEE-4X vacuum evaporator.

X-ray diffraction analysis (XRD)

In order to determine the mineralogical composition of the plaster layers, the collected samples were ground into powder in an agate mortar and were studied by X-ray powder diffraction using a Philips PW1710 diffractometer with Ni-filtered Cu–K_α radiation on randomly oriented samples. The counting statistics of the X-ray diffraction method were as follows: step size, 0.01° 2θ; start angle, 3°; end angle, 63°; and scan speed, 0.02° 2θ per second. Quantitative estimates of the abundance of the mineral phases were derived from the XRD data, using the intensity of certain reflections and external standard mixtures of minerals. The detection limit was ±2% w/w.

Infrared spectroscopy

The FT–IR technique offers a quick analysis of microsamples (less than 0.5 mg) (Bitossi *et al*. 2005). A small amount of the samples was removed and mixed with a KBr powder (~150 mg). After grinding, the mixture was pressed in an evacuated die in order to produce a pellet. FT–IR spectra were collected using a PerkinElmer Spectrum One FT–IR Spectrometer, in transmittance mode, over a wavenumber range of 4000 to 400 cm^{-1} at a resolution of 4 cm^{-1}.

RESULTS

The quantitative oxide analysis (wt%) of the studied samples, obtained by SEM–EDS, and the mineralogical composition determined by the XRD method are given in Tables 1 and 2, respectively.

Optical examination

Figure 2 illustrates stereomicroscopic images obtained on the examined plasters. In respect of the visual observation of the stratigraphical structure of the plasters (Fig. 2 (a)), it was clear that the layers are characterized by a stiff structure and they are easily distinguishable. Micro/macro-shrinkage cracks in the plasters' matrices were also frequently observed. The wall is first prepared with a base coat, the '*arriccio*', the thickness of which ranges from 100 to 300 μm. The coarse

Table 1 *Quantitative SEM–EDS analysis (compound %) of the studied samples*

Sample/Oxide	Na_2O	*MgO*	Al_2O_3	SiO_2	SO_3	P_2O_5	K_2O	*CaO*	Fe_2O_3	*PbO*	*BaO*
Fine plaster	–	–	3.58	4.60	–	–	–	91.82	–	–	–
	1.54	1.86	–	6.83	–	–	1.98	86.05	1.74	–	–
	–	2.23	2.43	4.56	–	–	–	88.24	2.54	–	–
Coarse plaster	3.03	–	2.20	42.42	–	–	2.65	49.70	–	–	–
	1.37	–	3.21	87.29	–	–	2.02	6.11	–	–	–
	1.63	1.54	2.17	4.41	23.40	–	–	28.12	–	–	38.73
Red pigment	1.65	–	1.90	4.28	–	–	–	16.41	75.76	–	–
Yellow pigment	–	–	2.06	14.24	–	20.48	1.34	24.95	5.64	31.29	–
Black pigment	0.85	2.06	0.91	1.00	–	47.12	–	48.06	–	–	–
White pigment	–	–	–	1.38	–	–	–	98.62	–	–	–

Table 2 *The mineralogical composition of the studied samples*

Sample/Component	*C*	*Q*	*Ar*	*V*	*Kf*	*Pl*	*He*	*Go*	*Cl*	*Hy*	*Ba*
Fine plaster	+++	+	–	–	–	–	–	–	–	–	–
	+++	+	–	–	+	+	–	–	–	–	–
	+++	+	–	–	–	+	–	–	–	–	–
Coarse plaster	+++	++	–	+	+	+	–	–	–	–	–
	++	++	–	–	–	+	–	–	–	–	+
	++	++	–	+	+	+	–	–	–	–	+
Red pigment	++	+++	–	–	+	–	+	–	+	–	–
Yellow pigment	+++	++	–	–	+		–	+	+	+	–
White pigment	+++	+	++	–	–	–	–	–	–	–	–

C = calcite; Q = quartz; Ar = aragonite; V = vaterite; Kf = feldspar; Pl = plagioclase; He = hematite; Go = goethite; Cl = clay minerals; Hy = hydrocerussite; Ba = barite. – = not determined; + = traces; ++ = minor constituent; +++ = major constituent.

plaster (Fig. 2 (b)) is based mainly on lime and siliceous aggregates of local sands from the River Nile. This layer is applied directly on to a second thin layer of finer, smoother lime plaster, the '*intonaco*'. The '*intonaco*' layer is based mainly on lime, with a thickness ranging from 150 to 200 μm; this layer is applied in sections over the coarse plaster. In some areas, pottery sherds (approx. 3 cm broad and 1.5 cm thick; see Fig. 2 (c)) were observed beneath the plaster layers. These sherds were probably used on purpose to achieve a good resistance to water and to prevent the cracking of the thickly layered plaster. The optical examination of the red pictorial layer shows traces of red grains diffused into the substrate, particularly at the surface (Fig. 2 (d)). In the case of the yellow pictorial layer, different yellow and green particles with different hollows on the surface are observed (Fig. 2 (e)). The microscopic examination of the black pictorial layer shows fine-grained particles of the pigment, while large grains of quartz are also noticeable (Fig. 2 (f)).

BSE–EDS results

The backscattered electron images (BSE) obtained on the outer surface are given in Figure 3. The BSE image of the fine plaster (Fig. 3 (a)) shows that the coarse siliceous aggregates are

Figure 2 *Stereomicroscopic images of the studied plaster layers. (a) A stratigraphical section in the plaster layers. (b) A close-up of the coarse plaster layer. (c) A cross-section in a plaster layer shows the pottery sherd brick embedded in the plaster layers. (d) A superficial image of the red pictorial layer. (e) A detail of the yellow pictorial layer. (f) A detail of the black pictorial layer.*

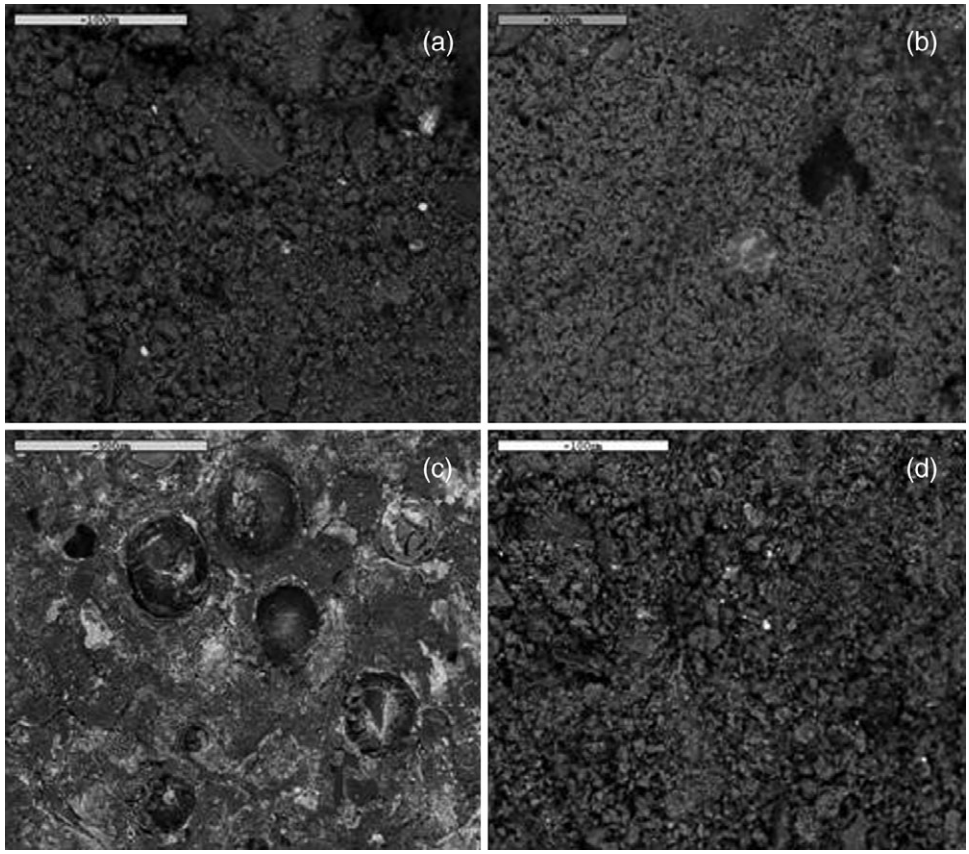

Figure 3 *BSE images obtained on the outer surfaces of the plaster layers: (a) the fine plaster layer; (b) the red pigment; (c) the yellow pigment; (d) the black pigment.*

distributed in a heterogeneous calcareous matrix. EDS microanalysis of the fine plaster shows a high proportion of calcium (Ca) as the major ion contained, which refers to the existence of calcium carbonates. Minor amounts of silicon (Si) and aluminium (Al) were found, while traces of magnesium (Mg), iron (Fe) and sodium (Na) were also detected. Moreover, further microanalysis of several spots on the plaster's surface showed that calcium carbonate always had been used. The silicon detected in the samples is due to fine siliceous aggregates of sand. EDS microanalysis of the coarse plaster shows that silicon and calcium are found as major ions. The spot microanalysis of the pink cementing grains that are distributed within the plaster matrix revealed the presence of sulphur (S) (13.44 wt%) and barium (Ba) (10.89 wt%). These grains were identified as barite, as confirmed by XRD measurements. Barite, or baryte (barium sulphate, $BaSO_4$) is generally found in sedimentary rocks. The presence of barite may be strictly accidental (as cement of the quartz from the geological source of this material).

The BSE image obtained from the red pigment sample shows granular aggregate particles of the red ochre scattered in the carbonate matrix (Fig. 3 (b)). EDS microanalysis of the sample shows that the peak for iron (28.41%) is present, which indicates the existence of iron oxide (probably hematite, Fe_2O_3) as a possible colouring material. Minor elements of calcium and

sodium were also detected, while the comparably low concentrations of silicon and aluminium indicate the possible existence of an aluminosilicate material (Zorba *et al*. 2007). The BSE image obtained on the outer surface of the yellow pigment sample (Fig. 3 (c)) shows a massive matrix with circular cavities. EDS microanalysis of the sample reveals the presence of calcium (Ca), phosphorus (P), lead (Pb) and iron (Fe) as the main ions contained in the pictorial layer. The peak for iron indicates the existence of iron oxide (probably goethite, FeOOH)—which is also confirmed from XRD analysis—while the detection of lead probably reveals the use of lead white, a basic lead carbonate (hydrocerussite, $Pb_3(CO_3)_2(OH)_2$). The BSE image of the black pigment shows different aggregates scattered in the calcareous matrix (Fig. 3 (d)). EDS microanalysis of the sample shows the detection of a high content of carbon, with calcium and phosphorus as the major ions present. Minor elements of magnesium, silicon, aluminium and sodium were also detected. Calcium (Ca) and phosphorus (P) are characteristic of bone (and ivory) black.

Mineralogical characterization

Representative XRD patterns of the studied plasters are shown in Figure 4. XRD patterns of the fine plaster samples (Fig. 4 (a)) indicate calcium carbonate (calcite, $CaCO_3$, 98%) as the predominant phase in the sample. Traces of quartz (SiO_2, 2%) were also detected in the sample. XRD measurements of additional plaster samples showed the presence of plagioclase (albite, $NaAlSi_3O_8$) and potassium feldspar (microcline, $KAlSi_3O_8$). XRD patterns of the coarse plaster samples (Fig. 4 (b)) showed that calcite (48%) and quartz (44%) are the main components of the sample. Traces of vaterite (a rare hexagonal polymorph of $CaCO_3$, 2%), potassium feldspar (microcline, 2%), plagioclase (albite, 2%) and barite (2%) were also found. XRD patterns of the red pigment sample showed that quartz (76%) is the main component, with minor amounts of calcite (18%). Traces of hematite (2%), plagioclase (2%) and clay minerals (2%) were also detected. XRD patterns of the yellow pigment sample showed that calcite (80%) is the main component; with minor amounts of quartz (9%). Traces of goethite (3%), potassium feldspar (2%), hydrocerussite (2%), graphite (2%) and clay minerals (2%) were also found. XRD patterns of the white pigment showed that calcite (68%) is the main component, with minor amounts of aragonite (30%), while traces of quartz (2%) were also found. This suggests that a mixture of calcite and aragonite was used to produce the white pigment. Consequently, we propose that ground shells were used to produce the pigment.

FT–IR results

Figure 5 displays an FT–IR spectrum obtained on the white pigment sample. The characteristic bands of calcite are present; the sharp one at 874 cm^{-1} is due to its asymmetric bending. The other calcite-related signals are the bands at 1450 and 713 cm^{-1} and the weak peaks at 1795 and 2517 cm^{-1}, which are combination and overtone bands (Baraldi *et al*. 2006). The bands at 699, 856 and 1083 cm^{-1} are attributed to aragonite (rhombic). According to Chakrabarty and Mahapatra (1999), aragonite displays a characteristic symmetric carbonate stretching vibration ($v1$) at 1083 cm^{-1} and a carbonate out-of plane bending vibration ($v2$) at 854 cm^{-1} in its FT–IR spectrum. The bands at ~400–475 cm^{-1} indicate the presence of amorphous silicates, probably attributed to the pozzolanic additives (e.g., pottery sherds) in the lime plasters. The pozzolanic additives used in the plaster layers are discussed below.

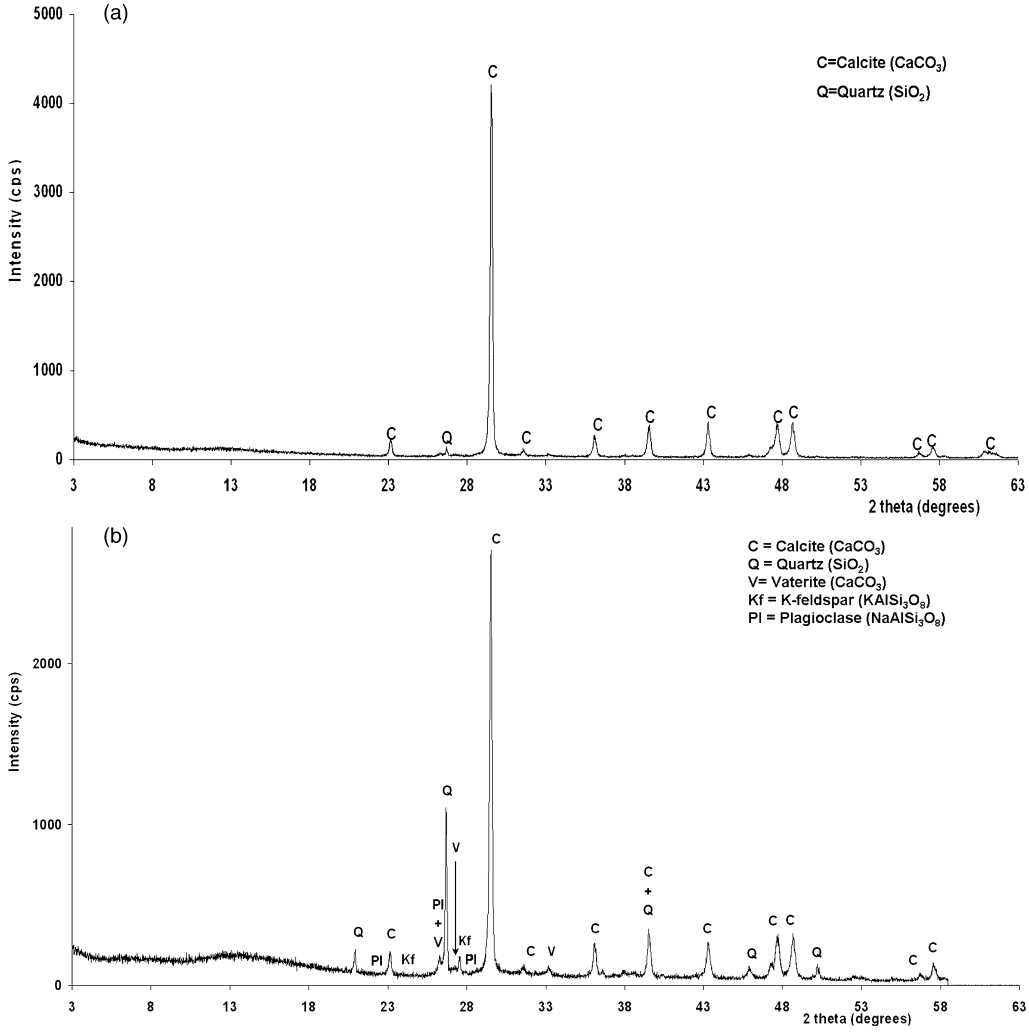

Figure 4 *Representative XRD patterns of the (a) fine and (b) coarse plaster layers.*

DISCUSSION

Plaster layers

The Egyptians employed both lime- and gypsum-based mortars in building the pyramids (2500 BC), the Greeks were using lime mortar in 500 BC and the Romans significantly refined hydraulic lime mortar in the second century BC (Dotter *et al*. 2009). As mentioned above, the stratigraphical analysis has shown that two layers of the plaster are clearly distinguishable. The first layer is made up of a lime wash with fine grains of silica sand; this layer had been thinned and polished carefully. The second layer is slightly thicker and was prepared from lime and large grains of silica sand. The mineralogical characterization by XRD of the studied samples confirmed that the

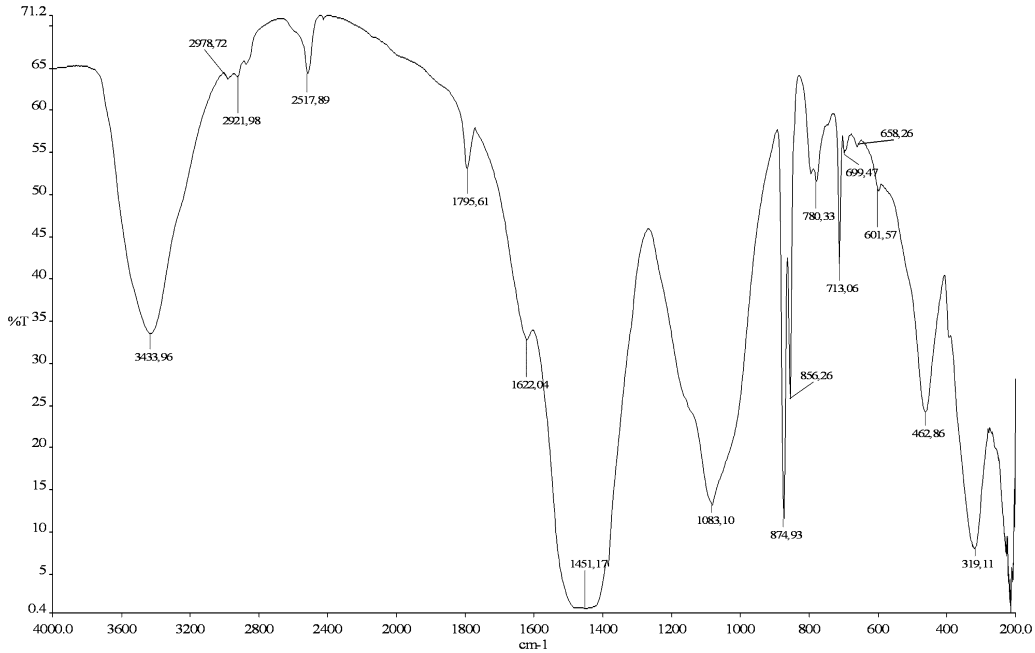

Figure 5 *The transmittance FT–IR (KBr) spectrum of the white pigment sample.*

plaster layers consist mainly of variable amounts of calcium carbonates (calcite and vaterite). Furthermore, EDS microanalysis revealed the presence of $CaO–SiO_2$, with minor amounts of Al_2O_3, MgO, Fe_2O_3 and K_2O. This suggests that a hydraulic lime, most probably originating from the calcination of impure limestone, was probably used to prepare the plaster layers. Vitruvius (1960), writing in the first century BC, recommended the use of a hydraulic mortar made of burned bricks and calcium hydroxide for damp rooms as the first '*arriccio*' layer. Calcium carbonate has three kinds of crystal polymorphs: calcite, aragonite and vaterite, with rhombohedral, orthorhombic and hexagonal structures, respectively (Lippmann 1973). Vaterite was identified by XRD in the coarse plaster samples. Vaterite is a rare hexagonal polymorph of $CaCO_3$, and crystallizes in the hexagonal system, in the dihexagonal bipyramidal class (Signorelli *et al*. 1996). According to McConnell (1960), vaterite has been quoted as a carbonation product of aged mortars incorporating hydraulic components. In addition to calcium carbonates, the sands and other basic component of the plasters came from river sources, because the sea-beach sands are not useful for building applications because of their salt content (Castriota *et al*. 2008). However, salts can easily be washed out, and then sea-beach sands could be used.

Pozzolanic additives

The use of pozzolans in mortars is said to have been initiated by the Greeks in 1500 BC (Velosa and Veiga 2005). The excellent properties of lime–pozzolana mortars, such as high strength, insolubility and hardening even under water, had been known to the ancient Roman builders since the third century BC (Sánchez-Moral *et al*. 2005). The hydraulic compounds are obtained from the reactions of $Ca(OH)_2$ with natural pozzolanes (natural earth of volcanic source) or artificial ones

(such as ground-fired bricks and tiles or ceramic shreds) (Franquelo *et al*. 2008). In our case, pottery sherds, crushed or finely ground bricks—called *Homra* in Arabic—were probably employed to improve the properties of the plaster layers, especially in the damp conditions. According to Böke *et al*. (2006), the bricks used as aggregates in the mortars and plasters from Ottoman bath buildings from Turkey have good pozzolanicity, which is mainly derived from their amorphous clay mineral dissociation products.

Red pigment

In all the cases, the pigments are supported in a lime wash (calcium carbonate). The red colour was obtained by using red ochre. EDS microanalysis showed the extensive existence of iron in great proportions. A small contribution of silicon and aluminium may indicate the presence of aluminosilicate materials (e.g., clays). It is well known that artists always add clay to iron oxide pigments to give them volume and adhesion; this is really very typical on wall paintings of almost all ages. Clays generally of the kaolin group and quartz are by far the most commonly found accessory minerals in the red/yellow earths and are also often found in earth pigments (Zorba *et al*. 2007).

Yellow pigment

In the yellow pigment samples, XRD data confirmed the presence of goethite for the yellow colour, and the EDS microanalysis showed that the peak for iron is present. A special green hue was produced by mixing goethite with lead white and bone black in different proportions. Lead white is one of the oldest human-made pigments, and the history of the synthetic one dates back to ancient Greece. Its mineral composition is generally considered to be hydrocerussite (Welcomme *et al*. 2007), although the incompatibility of lead white with the '*fresco*' technique seems to have been known and its use avoided (Kakoulli 2002). Lead white is unsuitable as a pigment in wet plasters and also it would react with air and discolour. The detected phosphorus is probably derived from calcium phosphate minerals ($Ca_3(PO_4)_2$), such as those found in bone.

Black pigment

The black pictorial surface was probably obtained by using bone black. Calcium (Ca) and phosphorus (P), detected by EDS microanalysis, are characteristic of bone (and ivory) black. The atomic mass ratio of magnesium to calcium in ivory is around 1:8, which is twice as high as in the bone (Freund 2002). On the basis of this ratio, the black pigment is concluded to be bone black and not ivory black (van Loon and Boon 2004). Bone black is one of the oldest pigments known to humans, and was originally made by charring animal bones; it has a blue–black colour. Besides carbon, it also contains calcium phosphate and carbonate, which have no colour value, but which improve the working quality and give a superior black colour (Mateo *et al*. 2009). Bone black is denser and much weaker in terms of tinting strength than either carbon or lampblack (Spengeman 1972, 160). Ivory black, on the other hand, is made from charred ivory (elephant tusks), which, unlike bone, has a relatively high magnesium content.

White pigment

From the XRD and FT–IR analyses, the white pigment was identified as a mixture of calcite and aragonite. Aragonite (a rhombic polymorph of $CaCO_3$) is rare, and other carbonate minerals are

largely confined to very special deposits such as evaporites or iron formations, or are present as trace minerals (Morse and Mackenzie 1990). Aragonite is formed by biological and physical processes, including precipitation from marine and freshwater environments. According to Bläuer-Böhm and Jägers (1996), calcium carbonate can also be present in the form of aragonite probably belonging to the binder, if the mortar has reached high temperatures during setting. Mazzocchin *et al*. (2010) reported that precious white pigments containing large amounts of aragonite were imported from Greece and Egypt in the period of the second century AD. Aragonite was probably used as a white pigment in Roman age wall paintings because of its higher hiding power, in comparison with calcite (Baraldi *et al*. 2007). The existence of aragonite in samples from the Roman age has also been reported by other authors (Mazzocchin *et al*. 2004, 2006, 2007, 2010; Duran *et al*. 2010).

Painting technique

We did not clearly identify the organic binders in the studied samples, and the continuous occurrence of calcium carbonates in the plaster layers, detected by XRD and FT–IR analyses, suggests the use of the '*fresco*' technique. Fresco is an ancient technique for painting on walls in which the original pigment is applied to a damp lime plaster and, after drying, the grains of pigments are clearly seen to be diffusing into a calcareous matrix (Marey Mahmoud 2009).

CONCLUSIONS

The application of different analytical techniques (namely, OM, SEM–EDS, XRD and FT–IR) was an attempt to answer some questions concerning materials used in the Ptolemaic baths recently discovered in front of the Karnak temple complex, Upper Egypt. The results showed that the plaster layers used in the Ptolemaic baths are based mainly on the use of lime. Pozzolanic additives such as pottery sherds and ground-fired bricks were used to improve the durability of the plasters to water. The results indicated that calcite is the predominant phase found in the fine '*intonaco*' plaster. The coarse '*arriccio*' plaster consists mainly of silica sand and two phases of calcium carbonates (calcite and vaterite). The chromatic palette used for decorating the plasters is based mainly on earth pigments. The red pigment was identified as red ochre, and the yellow pigment as goethite. A mixture of goethite, basic lead carbonate (hydrocerussite) and bone black in different proportions was used to produce a special green hue in the yellow pictorial layer. The black pigment was identified as bone black, and the white pigment was obtained through a mixture of calcite and aragonite. No significant differences were found between the preparation technique of the plaster layers in the Ptolemaic age and those used in the ancient Egyptian wall paintings, and their stratigraphy is almost the same. The combined results from XRD and FT–IR analyses showed the continuous detection of calcium carbonates in all the examined samples, with the high concentration of calcium in EDS microanalysis verifying the use of the '*fresco*' technique. In conclusion, further investigation of additional plaster samples will be of importance to improve the knowledge of the materials used in the Ptolemaic era in Egypt. The results will be used in the conservation–restoration interventions regarding these baths, and in particular, when applying injection grouts on the detached plaster layers.

ACKNOWLEDGEMENTS

The authors are grateful to Mr M. Bouriak, general supervisor of antiquities in Luxor, at the Supreme Council of Antiquities of Egypt (SCA), for his kind permission to collect the samples.

REFERENCES

Abd El Hady, M. M., 2000, The deterioration of Nubian sandstone blocks in the Ptolemaic temples in Upper Egypt, in *Proceedings of the 9th International Congress on Deterioration and Conservation of Stone, Venice, June 19–24, 2000*, vol. 2 (ed. V. Fassina), 783–92, Elsevier, Amsterdam.

Ali, M. F., 2003, Comparison study of blue and green pigments from the third intermediate period till the Greek Roman period, *Egyptian Journal of Analytical Chemistry*, **12**, 21–30.

Ashton, S.-A., 2008, Ptolemaic and Roman Memphis as a production center, in *Archaeology, history and science: integrating approaches to ancient materials* (eds. M. Martinón-Torres and Th. Rehren), 111–15, Left Coast Press, Walnut Creek, CA.

Baraldi, P., Baraldi, C., Curina, R., Tassi, L., and Zannini, P., 2007, A micro-Raman archaeometric approach to Roman wall paintings, *Vibrational Spectroscopy*, **43**, 420–6.

Baraldi, P., Bonazzi, A., Gioedani, N., Paccagnella, F., and Zannini, P., 2006, Analytical characterization of Roman plasters of the '*Domus Farini*' in Modena, *Archaeometry*, **48**, 481–99.

Bitossi, G., Giorgi, R., Mauro, M., Salvadori, B., and Dei, D., 2005, Spectroscopic techniques in cultural heritage conservation: a survey, *Applied Spectroscopy Reviews*, **40**, 187–228.

Bläuer-Böhm, Ch., and Jägers, E., 1996, Analysis and recognition of dolomitic lime mortars, in *Proceedings of the International Workshop on Roman Wall Painting, Roman Wall Painting Materials, Techniques, Analysis and Conservation, Fribourg, March 7–9, 1996* (eds. H. Béarat, M. Fuchs, M. Maggetti and D. Paunier), 223–35, Institute of Mineralogy and Petrology, Fribourg University.

Blyth, E., 2006, *Karnak: evolution of a temple*, Routledge, New York.

Böke, H., Akkurt, S., İpekoğlu, B., and Uğurlu, E., 2006, Characteristics of brick used as aggregate in historic brick–lime mortars and plasters, *Cement and Concrete Research*, **36**, 1115–22.

Bunbury, J. M., Graham, A., and Hunter, M. A., 2008, Stratigraphic landscape analysis: charting the Holocene movements of the Nile at Karnak through Ancient Egyptian time, *Geoarchaeology*, **23**(3), 351–73.

Castriota, M., Cosco, V., Barone, T., De Santo, G., Carafa, P., and Cazzanelli, E., 2008, Micro-Raman characterizations of Pompei's mortars, *Journal of Raman Spectroscopy*, **39**(2), 295–301.

Chakrabarty, P., and Mahapatra, S., 1999, Aragonite crystals with unconventional morphologies, *Journal of Materials Chemistry*, **9**, 2953–7.

Dotter, K. R., Smith, B. J., McAlister, J., and Curran, J., 2009, Sacrifice and rebirth: the history of lime mortar in the north of Ireland, in *Proceedings of the Third International Congress on Construction History, Brandenburg University of Technology Cottbus, Germany, May 20–24, 2009* (eds. K.-E. Kurrer, W. Lorenz and V. Wetzk), 499–506, NEUNPLUS1, Berlin.

Duran, A., Jimenez De Haro, M. C., Perez-Rodriguez, J. L., Franquelo, M. L., Herrera, L. K., and Justo, A., 2010, Determination of pigments and binders in Pompeian paintings using synchrotron radiation – high-resolution X-ray power diffraction and conventional spectroscopy–chromatography, *Archaeometry*, **52**, 286–307.

El Goresy, A., 2000, Polychromatic wall painting decorations in monuments of Pharaonic Egypt: compositions, chronology and painting techniques, in *Proceedings of the First International Symposium: 'The Wall Paintings of Thera'*, vol. I (ed. S. Sherratt), 49–70, Petros M. Nomikos and Thera Foundation, Piraeus, Athens, Greece.

Ellis, W. M., 1994, *Ptolemy of Egypt*, Routledge, New York.

Franquelo, M. L., Robador, M. D., Ramírez-Valle, V., Durán, A., Jiménez de Haro, M. C., and Pérez-Rodríguez, J. L., 2008, Roman ceramics of hydraulic mortars used to build the Mithraeum house of Mérida (Spain), *Journal of Thermal Analysis and Calorimetry*, **92**(1), 331–5.

Freund, A., 2002, On the occurrence of magnesium phosphates on ivory, *Studies in Conservation*, **47**, 155–60.

Gabolde, L., 2000, Origines d'Amon et origines de Karnak. Égypte, *Afrique et Orient*, **16**, 3–12.

Gabolde, L., Carlotti, J.-F., and Czerny, E., 1999, Aux origines de Karnak: les recherches récentes dans la 'cour du Moyen Empire', *Bulletin de la Société d'Égyptologie Genève*, **23**, 31–49.

Kakoulli, I., 2002, Late Classical and Hellenistic painting techniques and materials: a review of the technical literature, *Reviews in Conservation*, **3**, 56–67.

Kieser, J., Dennison, J., Anson, D., Doyle, T., and Laing, R., 2004, Spiral computed tomographic study of a pre-Ptolemaic Egyptian mummy, *Anthropological Science*, **112**, 91–6.

Lippmann, F., 1973, *Sedimentary carbonate minerals*, Springer-Verlag, Berlin.

Mao, Y., 2001, A technical examination of three Ptolemaic faience vessels, *The Journal of the Walters Art Museum*, **59**, 17–22.

Marey Mahmoud, H. H., 2009, *Study of the chromatic changes of the ancient pigments in some wall paintings in Egypt and the procedures of conservation*, unpublished Ph.D. thesis, Aristotle University of Thessaloniki, Greece.

Mateo, M. P., Ctvrtnickova, T., and Nicolas, G., 2009, Characterization of pigments used in painting by means of laser-induced plasma and attenuated total reflectance FTIR spectroscopy, *Applied Surface Science*, **255**, 5172–6.

Mazzocchin, G. A., Agnoli, F., and Salvadori, M., 2004, Analysis of Roman age wall paintings, *Talanta*, **64**, 732–41.

Mazzocchin, G. A., Del Faveroi, M., and Tasca, G., 2007, Analysis of pigments from Roman wall paintings in the 'Agro Centuriato' of Julia Concordia (Italy), *Annali di Chimica*, **97**, 905–13.

Mazzocchin, G. A., Orsega, E. F., Baraldi, P., and Zannini, P., 2006, Aragonite in Roman wall paintings of the VIII^{a} Regio, Aemilia, and X^{a} Regio, Venetia Et Histria, *Annali di Chimica*, **96**(7–8), 377–87.

Mazzocchin, G. A., Vianello, A., Minghelli, S., and Rudello, D., 2010, Analysis of Roman wall paintings from the Thermae of 'Iulia Concordia', *Archaeometry*, **52**, 644–55.

McConnell, J. D. C., 1960, Vaterite from Ballycraigy, Larne, Northern Ireland, *Mineralogical Magazine*, **32**, 535–45.

McKenzie, J., 2007, *The architecture of Alexandria and Egypt 300 B.C. – A.D. 700*, Yale University Press, Hong Kong.

Morse, J. W., and Mackenzie, F. T., 1990, *Geochemistry of sedimentary carbonates*, Elsevier, Amsterdam.

Sánchez-Moral, S., Luque, L., Cañaveras, J.-C., Soler, V., Garcia-Guinea, J., and Aparicio, A., 2005, Lime pozzolana mortars in Roman catacombs: composition, structures and restoration, *Cement and Concrete Research*, **35**, 1555–65.

Shortland, A. J., and Tite, M. S., 2005, Technological study of Ptolemaic – Early Roman faience from Memphis, Egypt, *Archaeometry*, **47**, 31–46.

Signorelli, S., Peroni, C., Camaiti, M., and Fratini, F., 1996, The presence of vaterite in bonding mortars of marble inlays from Florence Cathedral, *Mineralogical Magazine*, **60**, 663–5.

Spengeman, W. F., 1972, Pigments, in *Paint testing manual: physical and chemical examination of paints, varnishes, lacquers, and colors*, 13th edn (ed. G. G. Sward), 150–64, American Society for Testing Materials, Philadelphia, PA.

Tchapla, A., Méjanelle, Ph., Bleton, J., and Goursaud, S., 2004, Characterisation of embalming materials of a mummy of the Ptolemaic era: comparison with balms from mummies of different eras, *Journal of Separation Science*, **27**(3), 217–34.

van Loon, A., and Boon, J. J., 2004, Characterization of the deterioration of bone black in the 17th century *Oranjezaal* paintings using electron-microscopic and micro-spectroscopic imaging techniques, *Spectrochimica Acta Part B*, **59**, 1601–9.

Velosa, A. L., and Veiga, M. R., 2005, Pozzolanic materials—evolution mechanical properties, in *International Building Lime Symposium, Orlando, Florida, March 9–11, 2005*, 1–8.

Vitruvius, 1960, *The ten books on architecture VII*, transl. N. H. Morgan, 1st THUS edn, Dover Publications, New York.

Welcomme, E., Walter, P., Bleuet, P., Hodeau, J. L., Dooryhee, E., and Martinetto, P., 2007, Classification of lead white pigments using synchrotron radiation micro X-ray diffraction, *Applied Physics A*, **89**, 825–32.

Zorba, T., Andrikopoulos, K. S., Paraskevopoulos, K. M., Pavlidou, E., Popkonstantinov, K., Kostova, R., Platnyov, V., and Sister Danillia, 2007, Infrared and Raman vibrational spectroscopies reveal the palette of frescos found in the medieval monastery of Karaach Teke, *Annali di Chimica*, **97**, 491–503.